Statistical Analysis of Methane Detonation Wave Structure in a Narrow Channel

Mark D. Frederick[*1], Rohan M. Gejji[†1], Joseph E. Shepherd[‡2], and Carson D. Slabaugh[§1]

[1]*Purdue University, West Lafayette, IN 47907*
[2]*California Institute of Technology, Pasadena, CA 91225*

Multi MHz schlieren measurements are performed of methane-oxygen 2D planar detonations diluted with between 20% and 33% nitrogen or argon. The 5 MHz temporal resolution provided by these images allows for key structures to be traced as they evolve. An edge tracking algorithm is developed and applied in order to compute the velocity of the leading front. A detailed velocity map is presented that shows the cellular structure of each detonation, similar to a soot foil, but also illustrates the dynamic evolution of the structure. Finally, kernel density estimates of the probability density function of front velocity and the first four moments are used to statistically describe the two-dimensional structure of unstable methane detonations.

I.   Introduction

The structure of an unsteady detonation front was first observed by White[1] and has since been the focus of numerous other studies.[2–8] The leading shock is not planar or steady, but rather exhibits spatially and temporally varying oscillations due to triple-point intersections with transverse waves within the reaction zone. Transverse wave motion is oriented perpendicular to the global direction of detonation wave propagation. Near the locus of collision (the triple point), a localized region of high enthalpy gas is generated due to heat release, which drives the incident shock forward. Following triple point passage, the gases behind the mach stem expand and the local wave speed decays until the passage of another triple point. This unsteady process occurs with a characteristic time-scale associated with the triple point intersections across the detonation front. The corresponding length scale is the detonation cell-size. The triple-point trajectories and intersection length scales along the channel wall can be measured using the soot foil technique. The stability of a given detonation can be qualitatively characterized based on the regularity and size of the cellular detonation structure and in some cases measured and quantitatively characterized.[9, 10] A schlieren image of a detonation with these key features called out is shown in figure 1.

For highly unstable detonations, such as those typically produced from hydrocarbon fuels,[8, 11] the soot foil becomes difficult to quantitatively interpret due to large range of scales that are characteristic of an unstable detonation. An alternative method, used by Austin et al.,[8] compares the relative stability of different mixtures by calculating the reduced activation energy $\theta = E_a/RT_{vN}$ and comparing it to the neutral stability boundary of Lee and Stewart.[12] Generally speaking, for mixtures with similar M_{CJ}, the higher the reduced activation energy, the higher the degree of instability. Using a detailed reaction mechanism to predict effective activation energy, this methodology can be used to rank order detonations in terms of predicted degree of instability and the results are generally consistent with observations on cellular structure. This notion was extended by Ng et al.[13] who demonstrated that the in addition to effective activation energy, the ratio of the width of the energy release zone to the induction zone length was a highly correlated with the observed degree of cellular regularity; the smaller this ratio, the more irregular the cellular structure.

---

[*]Graduate Research Fellow, School of Mechanical Engineering
[†]Research Engineer, School of Aeronautics and Astronautics
[‡]C. L. "Kelly" Johnson Professor, Graduate Aerospace Laboratories
[§]Assistant Professor, School of Aeronautics and Astronautics

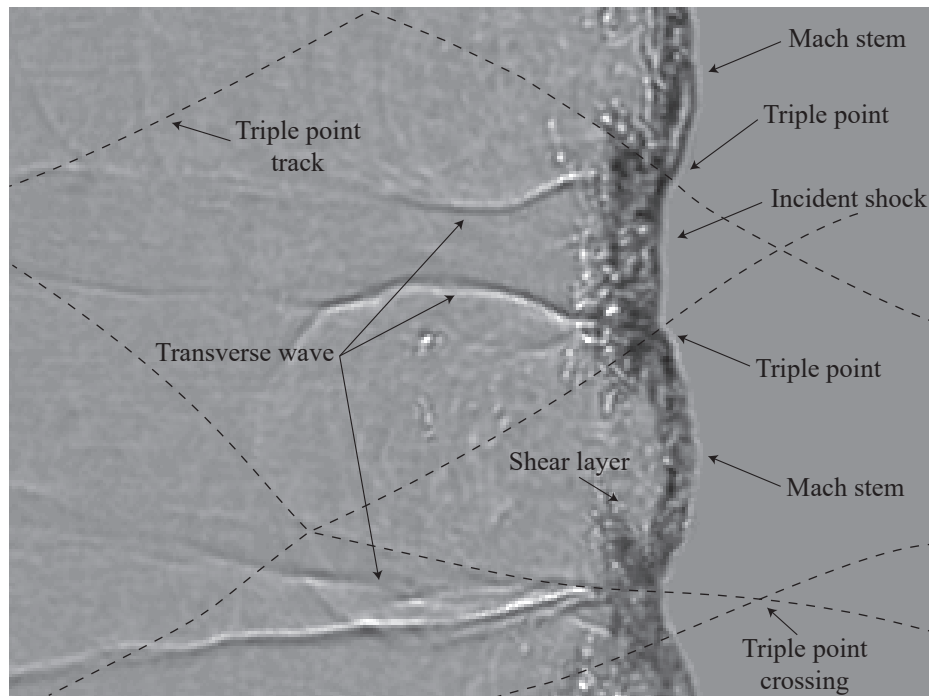American Institute of Aeronautics and Astronautics

Figure 1: Schlieren image of $CH_4 - 2O_2 - 1.5Ar$ detonation with key cell features labeled.

There have been a number of efforts to statistically analyze unstable detonation propagation using numerical simulation. Radulescu and coworkers[11,14,15] have statistically quantified instability in numerically-computed denotations by using both Euler and Navier-Stokes equations using modeling techniques developed for compressible turbulent flow simulation. Shepherd and Liang[16] analyzed Euler equation simulations to estimate relative and joint frequency distributions relating measured wave speed to measured induction length and determine how the distributions compare to the predictions of quasi-steady reaction zone structure.

The primary objective for this study is to statistically describe the two-dimensional structure of unstable methane detonations from experimental results. The experimental platform for this study is the GALCIT *Narrow Channel Facility* (NCF).[7] Substantial efforts have made in the past to characterize detonation instability experimentally using soot foils, but soot tracks primarily have only qualitative value except in the case of relatively stable mixtures with a regular pattern of instability. Hydrocarbon fuel detonations in oxygen or air are intrinsically unstable except at the highest level of Ar dilution and for quantitative evaluation, require more sophisticated techniques than soot foils. Due to the advent of ultra-high-speed digital imaging, experimental results can now approach the temporal and spatial resolution that could previously only be achieved with a simulation. MHz rate laser schlieren will be used to capture the density field. A statistical description of the velocity front will allow for the level of instability in highly unstable detonations to be quantified.

II.   Experiment Description

The *Narrow Channel Facility* (NCF) was developed by Austin[7] in the Explosion Dynamics Laboratory at Caltech to study the unstable structure in gaseous detonations . The NCF is a high aspect ratio, rectangular channel with a height of 152.4 mm width of 17.8 mm, and span of 4.2 m. The dimensions were chosen such that the width is nominally smaller than the detonation cell size for a targeted range of mixtures and test conditions. This configuration effectively suppresses transverse wave motion across the width of the channel, generating a two-dimensional detonation structure across the channel height that is conducive to the application of path-integrated optical diagnostics.

The reactant gases, typically one fuel, oxidizer, and inert, are introduced into the channel using the method of partial pressures. The loading process takes about 120 seconds and the reactants are circulated for an additional thirty seconds to ensure a homogeneous mixture. A K-type thermocouple and low frequency
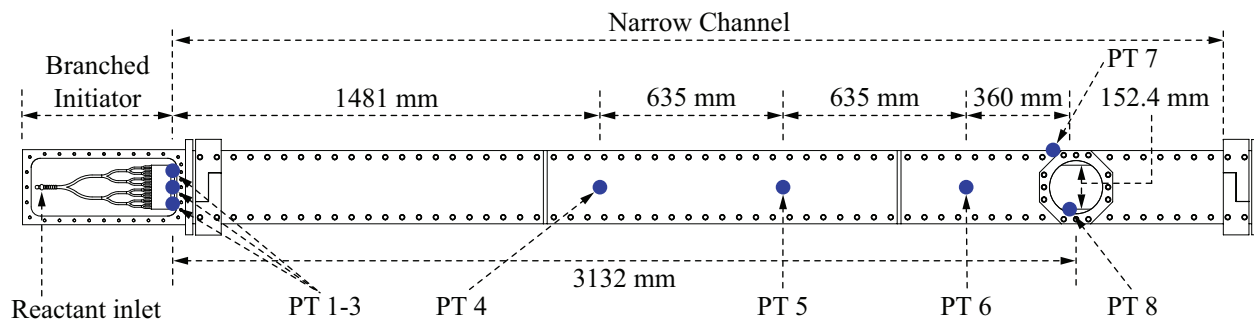
American Institute of Aeronautics and Astronautics

Figure 2: Experimental overview and dimensions. High frequency pressure measurement locations labeled as PT 1-8.

pressure transducer are placed just upstream of the branched initiator and are used to record the initial temperature and pressure. The planar detonation is driven by a branched initiator, designed by Jackson and Shepherd.[17] The initiator operates with an equimolar C_2H_2-O_2 mixture and is ignited with a spark plug. The facility is operated at low pressure (22 kPa) to have sufficiently large reaction zones in order to clearly observe the cellular structure.

Pressure fluctuations in the channel are recorded at six axially distributed locations using PCB 113B26 high-frequency dynamic pressure transducers (PT), installed flush with the channel wall, and sampled at 2 MHz. PT 1-3 monitor the planarity of the wave as it enters the test section. PT 4-8 are used to track the progression of the detonation wave as it traverses the channel by using the time of arrival method. These data can be used to monitor the detonation velocity and compare with the theoretical Chapman Jouguet velocity. Figure 2 identifies the location of all the high-frequency pressure measurement locations (PT 1-8). More details on the experimental procedure are available in Frederick *et al.*[18]

A Z-type schlieren system is used to obtain spatial information about the density field. Optical access is provided by 170 mm fused quartz windows located at the end of the channel, shown in figure 2. The
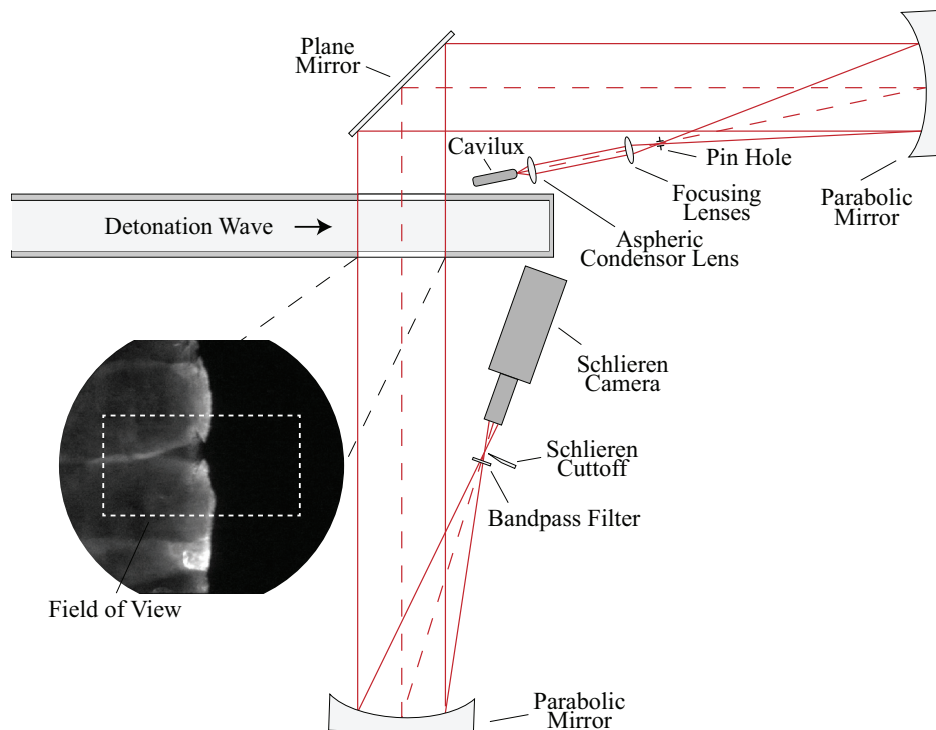

Figure 3: Schematic illustration of optical setup for Z-type schlieren measurements. Not to scale. The image illustrating the field of view is of CH* chemiluminescence from a methane detonation.

optical setup and imaging field of view are sketched in figure 3. In order to minimize motion blur without the use of an external gating device, the CAVILUX Smart UHS pulsed light source is used for the schlieren measurements. The CAVILUX produces incoherent 640 ± 6 nm light with a 10 ns pulse duration at a 5

American Institute of Aeronautics and Astronautics

MHz pulse frequency. An aspheric condenser lens is placed directly downstream of the light source and a series of lenses are used to set the divergence angle of the light, defined by the desired field of view and focal length of the parabolic mirror, before passing the focus of the beam through a pin-hole aperture to enforce a point source. Parabolic mirrors with f/10 are used to collimate and direct the light through the test section. The light passes through a 640/20 nm single-band bandpass filter to eliminate light emission from the detonation. A circular aperture is used as the schlieren cutoff. The resulting images are recorded on a Shimadzu HPV-X2. The field of view is 100 x 63 mm, depicted in figure 3. PT 7 is used to trigger the camera once it registers a pressure increase corresponding to the detonation wave passage. The camera records 256 images that track the propagation of the wave over the selected field of view.

III.   Results

Stoichiometric methane and oxygen mixtures with 20-33% nitrogen or argon dilution were studied in this work. Methane is a widely studied fuel and is of practical relevance for both gas turbine and rocket combustors.[11,19–29] Four different dilution percentages were chosen for each inert in order to vary the detonation structure, leading to eight test cases total. These are listed in table 1 along with various detonation parameters that were found using ZND calculations through the Shock and Detonation Toolbox.[30] The pressure and temperature for all cases was held constant at $P_0 = 22.27$ kPa and $T_0 = 302$ K. The mean relative velocity deficit $(U - U_{CJ})/U_{CJ}$ was calculated using PT 4-8 and varied between $\pm 5\%$ for all cases.

A time series of images for a representative case, $CH_4 - 2O_2 - 1.25N_2$, is shown in figure 4. Background subtraction and thresholding are performed to remove stationary gradients introduced by imperfections in the windows. For brevity, every fifth image captured during the test is presented. The time separation between each frame is consequently 1 μs. These images capture the evolution of multiple transverse shock waves and triple points on the main front, features characteristic of highly-unstable detonations.[7,8,11,16] The images begin with the growth of two mach stems, in the middle and bottom of frames (a)-(h). As these mach stems grow toward each other, the formation of shear layers, separating products and unburned reactants behind the wave front, are observed at each vertex of the shared incident shock. One of these is particularly evident at y = 25 mm of frame (h). Frames (i) and (j) show the triple point crossing as these two mach stems collide and generate a new mach stem in frame (k) (centered at y = 25 mm). The mach stem born out of frame (k) does not grow symmetrically. The triple point (TP) on either end collides with a neighboring TP at different times. First, the TP that moves downward collides in frame (x) at y ≈ 5 mm, as the new mach stem generated by this collision can be seen growing from frame y onward. Second, the TP that moves upward collides about 10 μs later in frame (z) at y ≈ 40 mm. As a result of these non-uniform collisions and irregularly-spaced transverse waves, the leading front lacks the organized and predictable wave shape characteristic of more stable detonations.[8] Frame (ad) shows a leading front with multiple kinks or inflection points that have transverse waves emanating of various strengths.

Table 1: Calculated detonation parameters at $P_0 = 22.27$ kPa and $T_0 = 302$ K. U_{CJ} is the Chapman-Jouguet velocity, Δ_I is the induction length, Δ_E is the exothermic length, θ is the reduced activation energy, and M_{CJ} is the Mach number. All parameters are found using ZND calculations in the Shock and Detonation Toolbox.[30]

Mixture	U_{CJ} [m/s]	Δ_I [mm]	Δ_E [mm]	θ	M_{CJ}	Label (fig. 5)
CH_4-$2O_2$-$0.75N_2$	2195	2.11	0.104	11.03	6.154	a
CH_4-$2O_2$-N_2	2163	2.54	0.110	11.20	6.067	b
CH_4-$2O_2$-$1.25N_2$	2134	3.04	0.128	11.36	5.987	c
CH_4-$2O_2$-$1.5N_2$	2107	3.60	0.140	11.52	5.915	d
CH_4-$2O_2$-$0.75Ar$	2137	1.11	0.085	10.26	6.185	e
CH_4-$2O_2$-Ar	2093	1.13	0.092	10.19	6.103	f
CH_4-$2O_2$-$1.25Ar$	2054	1.14	0.102	10.13	6.028	g
CH_4-$2O_2$-$1.5Ar$	2020	1.16	0.103	10.08	5.960	h

American Institute of Aeronautics and Astronautics

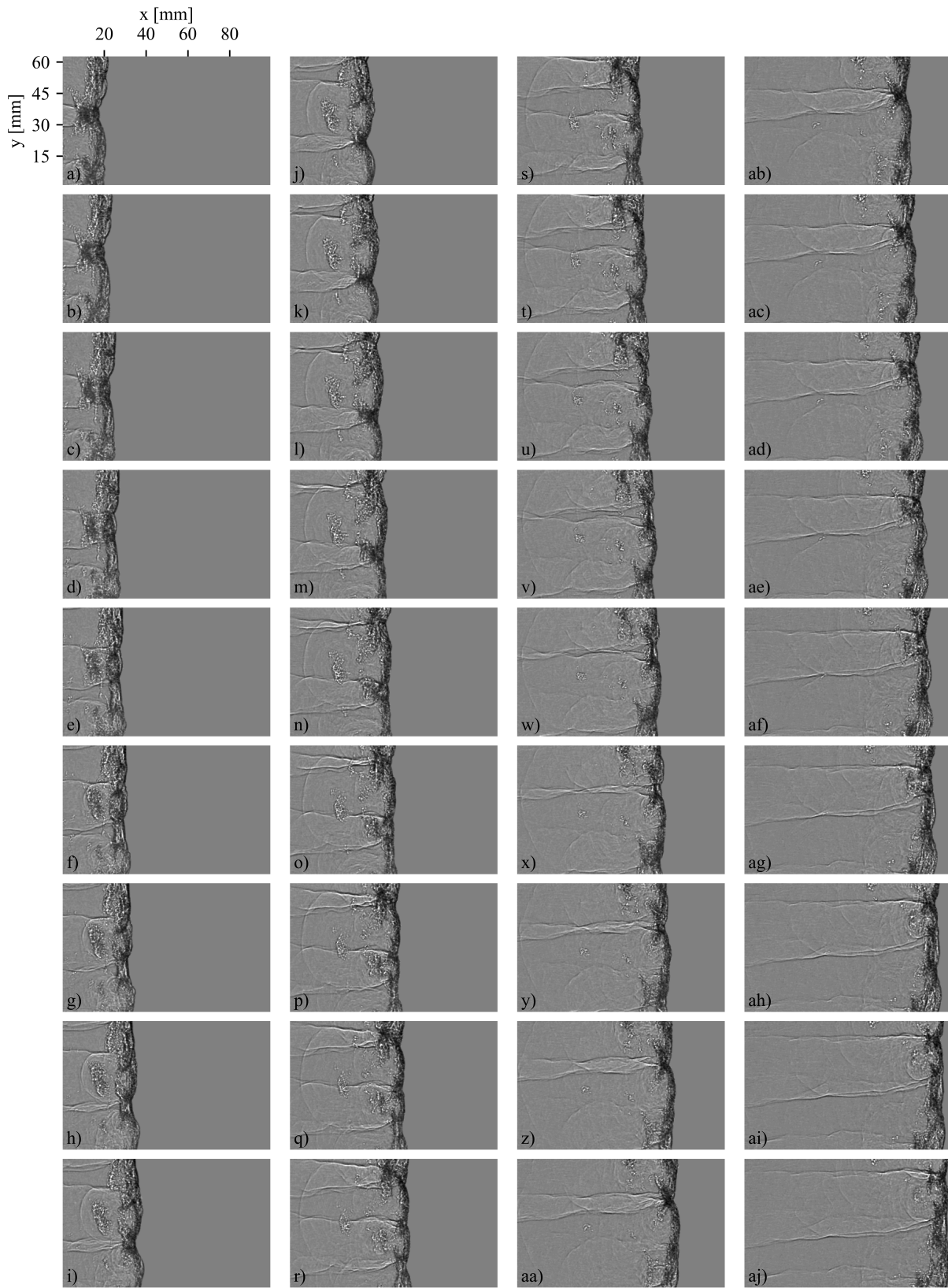**Figure 4:** Sequence of schlieren images of a CH_4-$2O_2$-$1.25N_2$ detonation. The time between images is 1 μs; every fifth image is shown. Each image is 100 x 63 mm.

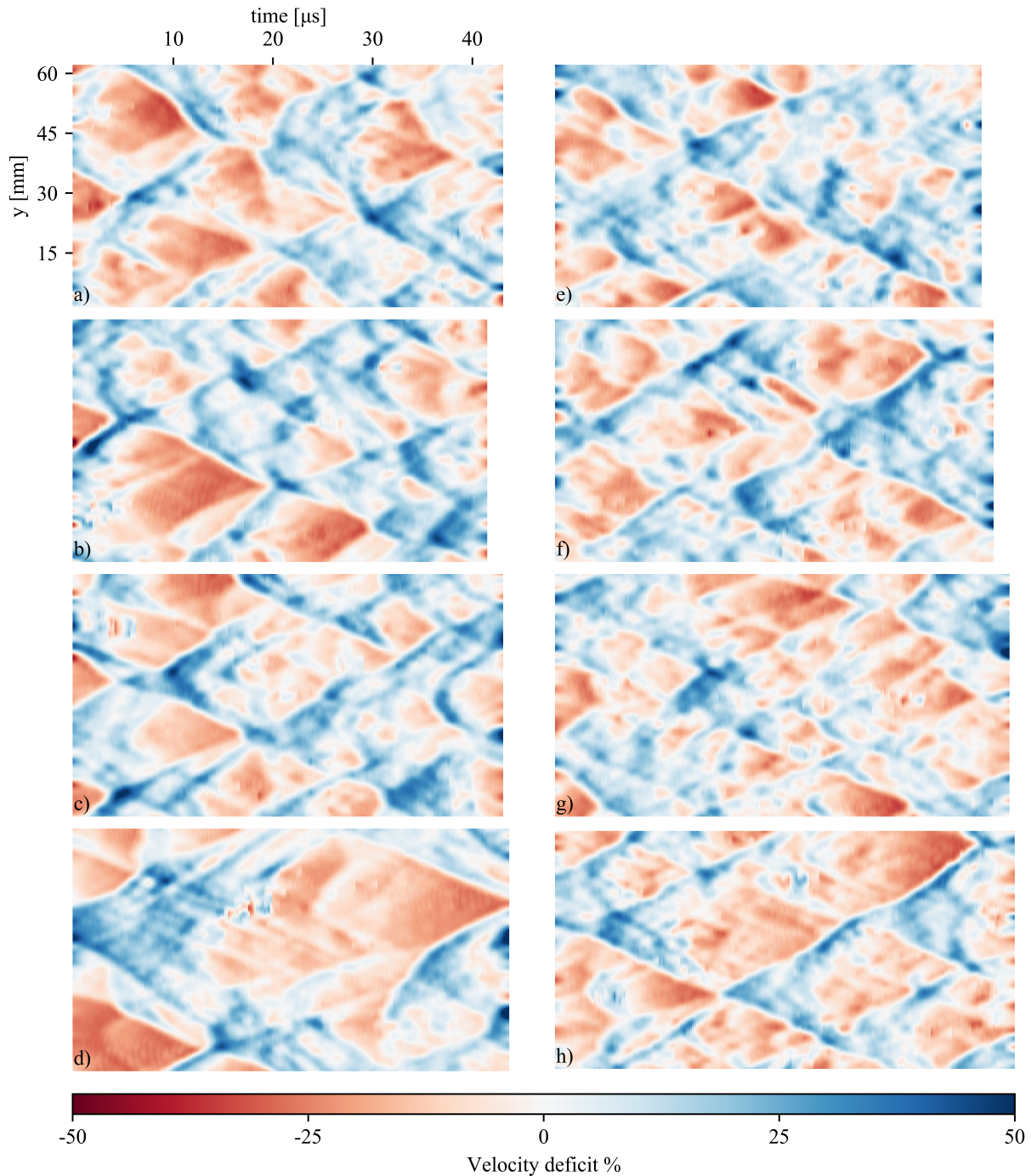American Institute of Aeronautics and Astronautics

Figure 5: Velocity deficit map of images for each case. The labels, (a)-(h), correspond to the cases listed in table 1.

Additionally present in these images is the evolution of other important features behind the front. Gases that are processed by incident shocks make it behind the leading front and exist in pockets. These pockets can be clearly seen $\approx$ 10 mm behind the leading front in frames (e) and (aa). These pockets have important implications as to how deflagrative burning behind the front aids in sustaining the detonation wave.[11, 16, 19, 31–35] These images show how the dissipation of these pockets occurs and the length of time they exist downstream of the front. In the case of the pocket beginning in frame (e), it does not fully dissipate until frame (ad), which is about 125 μs later. Another interesting feature that can be traced in time is the circular explosions that are produced at triple-point crossings and expand downstream into the product region. The most conspicuous one in figure 4 can first be seen in frame (g) as the half-circle that connects

American Institute of Aeronautics and Astronautics

the transverse waves on either side of the growing mach stem mid-frame. The weak shock produced can be seen weakening as the structure grows radially larger. Other circular explosions, on smaller scales, are also evident throughout this case and produce a wrinkled texture in the downstream region. These features appear similar to the localized explosions that were observed by Austin et al.[8] in highly unstable propane-oxygen-nitrogen detonations. The size and number of these explosions can be used to qualitatively describe the degree of instability of a mixture because the locus of each explosion is a point of intense reaction in the detonation.

The increased temporal resolution provided by imaging at 5 MHz allows for the dynamic spatial structure of the detonation to be captured quantitatively. Soot foils provide an indication of the extent of spatial organization of the transverse waves but are challenging to interpret quantitatively with statistical methods. The results presented in figure 5 captures the detonation wave front history in term of instantaneous velocity deficit, while also enabling characterization of the cellular structure in terms of size and regularity. To create these deficit maps, an algorithm was developed that combined the Sobel operator with active contour modeling[36] to identify and extract the leading front position in each image. Once the leading edge was extracted the horizontal velocity was calculated using a Savitzky-Golay[37] filter, choosing parameters to sufficiently smooth the data for presentation while retaining fidelity to the main time-dependent features.

Figure 5 shows a velocity deficit map for each of the cases listed in table 1. The nitrogen diluted cases are shown in the left column and the argon diluted cases are shown in the right. Dilution percent increases from top to bottom. Immediately evident is that these velocity deficit maps look very much like soot foils; a fish scale like shape outlines each cell. The results of figure 5c correspond with the images of figure 4 and the overall structure matches up well. The range of spatial scales present in all cases is made clear; none have a uniform cell size. Figure 5b shows a large cell with a width of ≈ 32 mm and small cells that are only a few mm wide. As expected, increasing dilute percentage increases cell size. The largest cells in 5a and 5e are ≈ 30 mm, while the largest cell in 5d is ≈ 60 mm and ≈ 45 mm in 5e.

The additional information gained from the velocity deficit map is how the velocity develops during the cell cycle. For example, figure 5d primarily shows the complete cycle of a large single cell. At the beginning of the cycle the Mach stem is moving faster than U_{CJ} until ≈ 15 μs. At this point (about 1/4 through the cell cycle) the speed of the Mach stem falls below U_{CJ} and then transitions to an incident shock at ≈ 25 μs. As the cell closes and the two Mach stems on the exterior of the cell converge, the incident shock decelerates to about 60% U_{CJ} before exiting the frame. The path of the lower triple point as the cell is closing in this case is also unique. In all other instances the triple point path, which moves at $\approx U_{CJ}$, is linear. However, in this case the triple point path is curved, indicating that the Mach stem is accelerating faster vertically than it is horizontally.

Turbulent flow analysis generally relies on statistical descriptions of instabilities due to the stochastic nature of these processes. Highly unstable detonations are turbulent flows, but due to a lack of high resolution experimental measurements in space and time a statistical approach has not been possible before now. Probability distributions of velocity have been calculated for simulated detonations[7, 11, 16] and show that the velocities along the front are skewed toward sub-CJ velocities. This is reconciled by fact that detonations spend more time at slower speeds because the Mach stem accelerates rapidly and the incident shock decelerates slowly. Figures 6a and 6b present estimates (using the kernel methodology) of the probability distribution function (PDF) of velocity deficits for the nitrogen and argon cases, respectively. The nitrogen-diluted cases, shown in figure 6a, have velocity deficit distributions that are nearly indistinguishable, despite changing the amount of dilution. The argon-diluted cases, shown in figure 6b, display a clearer sensitivity to varying levels of dilution. As the amount of diluent is decreased, the density distribution curves shift toward a higher normalized velocity. The 33% nitrogen- and argon-diluted cases are the only ones with a clear sub-CJ maximum probability. The 33% argon-diluted case is the clear outlier from the group, with a sharp peak occurring at a velocity deficit of about -12.5 %. Examining figure 5h, which correspond to this density curve, the reader can observe that there are relatively less regions of positive velocity deficit. The interpretation of these velocity deficit distributions is highly dependent on choice of the mean detonation velocity, which is different from the ideal value of U_{CJ}. Based on the velocity data obtained from the PTs, the overall speed of the wave is moving between 2% and 5% above U_{CJ}. If U_{CJ} were recast to the mean value as determine by the PTs, the velocity deficit probability distributions would shift such that the distribution favored sub-CJ speeds.

The first four moments of distribution for the plots shown in figure 6 can be analyzed to understand the symmetry properties of these cases. These moments are listed in table 2 for all cases. The mean and
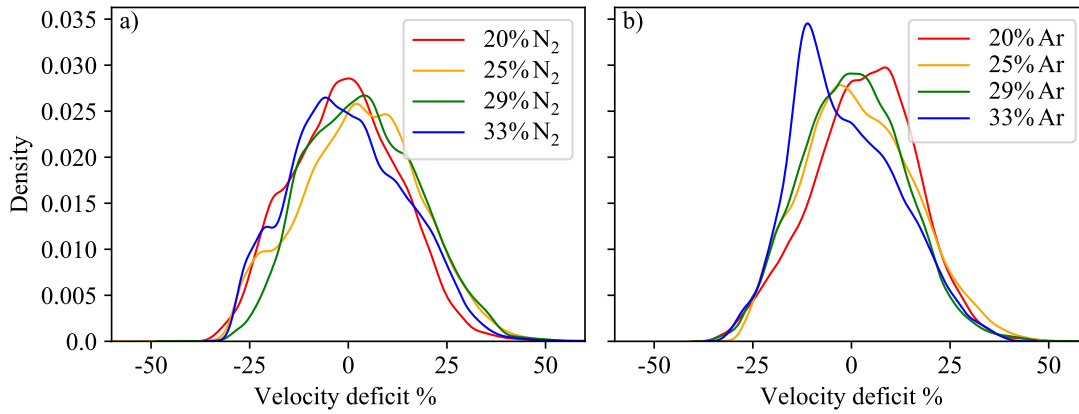
American Institute of Aeronautics and Astronautics

Figure 6: Kernel density estimate of velocity deficit PDF for nitrogen (a) and argon (b) diluted cases.

variance are both raw moments, meaning that their values are understood in the context of velocity deficit percent. Skewness and kurtosis are normalized by standard deviation and carry no dimensional significance. For all cases, the mean value is within 4% of U_{CJ}. The mean value of the argon-diluted cases decreases monotonically with increasing dilution. The variance, which measures the spread of a data set, is consistent within the nitrogen- and argon-diluted data sets. The argon-diluted cases have a slightly lower variance than the nitrogen-diluted cases, indicating that the velocity spread is smaller. This consistent with experimental observations and numerical simulations by previous investigators that argon dilution has a pronounced stabilizing effect on detonations. Skewness measures the asymmetry of the data and the sign of the skewness describes on which side of the distribution the tail is dominate. A positive skewness means that the tail on the right side is longer and the mass of the data is pushed toward the left; a negative skewness means the opposite. For the data considered here, all but one skewness value is positive. The indicates that for these cases velocities that occur at either extreme are more likely to be at speeds greater than U_{CJ}. Figure 6 clearly shows this trend in that the left tails of the curves abruptly end at a velocity deficit of about -30% and the right tails slowly converge to a velocity deficit of about 50%. Kurtosis,[38] like skewness, also deals with the tails of a distribution and measures how the tails compare to those of a Gaussian distribution. For these cases all but one kurtosis value is negative, which means that these mixtures have less outliers than a Gaussian curve and the velocity is less likely to experience an extreme value.

Table 2: The first four moments of distribution for the velocity data presented in figures 5 and 6.

Mixture	Mean	Variance	Skewness	Kurtosis
CH_4-$2O_2$-$0.75N_2$	-0.705	184.6	0.117	-0.363
CH_4-$2O_2$-N_2	2.987	225.9	0.022	-0.363
CH_4-$2O_2$-$1.25N_2$	3.777	196.5	0.228	-0.380
CH_4-$2O_2$-$1.5N_2$	0.115	214.6	0.296	-0.265
CH_4-$2O_2$-$0.75Ar$	3.153	173.4	-0.091	-0.082
CH_4-$2O_2$-Ar	2.119	192.6	0.278	-0.314
CH_4-$2O_2$-$1.25Ar$	0.526	169.6	0.199	0.015
CH_4-$2O_2$-$1.5Ar$	-1.357	176.6	0.394	-0.405

IV.   Conclusion

Due to their high degree of instability, methane detonations are challenging to quantitatively characterize by experiments using soot foils or single images. In this work methane detonations diluted with nitrogen and argon are studied experimentally using MHz-rate schlieren imaging. These images provide time-resolved insight about detonation features not observable on a soot foil, such as the consumption of unburned pockets that exist behind the wave front. Velocity maps of wave passage are presented that provide the spatial

information of a soot foil, but also the dynamic evolution of a main and transverse wave motion. These results led to a statistical description of the detonation front velocity that allowed for the effects of changing dilution to be analysed based on the symmetry properties of the velocity distributions. For the nitrogen diluted cases studied here, a significant statistical difference is not observed in the velocity distribution with the degree of dilution; the mean value being consistently located at U_{CJ} for the mixture. In contrast, the argon diluted cases show a clear trend in the statistics of the velocity deficit. As the degree of dilution increases from 20% to 33%, the peak of distribution is shifted from -12.5% to 15%. The shape of the velocity distributions for the 33% argon diluted case agrees with what has been previously published[7, 11, 16] using simulations and shows that wave is skewed toward sub-U_{CJ} values. However, for all other mixtures the distribution is observed to be centered around U_{CJ}. The simulations mentioned were not performed for the mixtures studied here and further investigation is required.

V. Acknowledgments

References

[1]White, D. R., "Turbulent structure of gaseous detonation," *Physics of Fluids*, Vol. 4, 1961, pp. 465–480.

[2]Tsuboi, N., Katoh, S., and Hayashi, A. K., "Three-dimensional numerical simulation for hydrogen/air detonation: Rectangular and diagonal structures," *Proceedings of the Combustion Institute*, Vol. 29, 2002, pp. 2783–2788.

[3]Gamezo, V. N., Poludnenko, A. Y., Oran, E. S., and Williams, F. A., "Transverse waves resulting from pulsating instability of two-dimensional flames," *Combustion and Flame*, Vol. 161, No. 4, 2014, pp. 950–957.

[4]Pintgen, F., Eckett, C. A., Austin, J. M., and Shepherd, J. E., "Direct observations of reaction zone structure in propagating detonations," *Combustion and Flame*, Vol. 133, No. 3, 2003, pp. 211–229.

[5]Mazaheri, K., Mahmoudi, Y., and Radulescu, M. I., "Diffusion and hydrodynamic instabilities in gaseous detonations," *Combustion and Flame*, Vol. 159, No. 6, 2012, pp. 2138–2154.

[6]Urtiew, P. A., "Idealized two-dimensional detonation waves in gaseous mixtures," *Acta Astronautica*, 1976.

[7]Austin, J. M., *The Role of Instability in Gaseous Detonation*, Ph.D. thesis, California Institute of Technology, 2003.

[8]Austin, J., Pintgen, F., and Shepherd, J., "Reaction zones in highly unstable detonations," *Proceedings of the Combustion Institute*, Vol. 30, No. 2, 2005, pp. 1849–1857.

[9]Austin, J. M. and Shepherd, J. E., "Detonations in hydrocarbon fuel blends," *Combustion and Flame*, Vol. 132, No. February 2002, 2003, pp. 73–90.

[10]Crane, J., Shi, X., Singh, A. V., Tao, Y., and Wang, H., "Isolating the effect of induction length on detonation structure: Hydrogen–oxygen detonation promoted by ozone," *Combustion and Flame*, Vol. 200, 2019, pp. 44–52.

[11]Radulescu, M. I., Sharpe, G. J., Law, C. K., and Lee, J. H., "The hydrodynamic structure of unstable cellular detonations," *Journal of Fluid Mechanics*, Vol. 580, 2007, pp. 31–81.

[12]Lee, H. and Stewart, D., "Calculation of linear detonation instability : one-dimensional instability of plane detonation," *J. Fluid Mech*, Vol. 216, 2020, pp. 103–132.

[13]Ng, H., Radulescu, M., Higgins, A., Nikiforakis, N., and Lee, J., "Numerical Investigation of the Instability for One-Dimensional Chapman-Jouguet Detonations with Chain-Branching Kinetics," *Combustion Theory and Modelling*, Vol. 9, No. 3, Aug. 2005, pp. 385–401.

[14]Maxwell, B. M., Bhattacharjee, R. R., Lau-Chapdelaine, S. S. M., Falle, S. A. E. G., Sharpe, G. J., and Radulescu, M. I., "Influence of Turbulent Fluctuations on Detonation Propagation," *J. Fluid Mech.*, Vol. 818, May 2017, pp. 646–696.

[15]Sharpe, G. J. and Radulescu, M. I., "Statistical Analysis of Cellular Detonation Dynamics from Numerical Simulations: One-Step Chemistry," *Combustion Theory and Modelling*, Vol. 15, No. 5, Oct. 2011, pp. 691–723.

[16]Shepherd, J. E., "Detonation in gases," *Proceedings of the Combustion Institute*, Vol. 32, No. 1, 2009, pp. 83–98.

[17]Jackson, S. I., Austin, J. M., and Shepherd, J. E., "Planar Detonation Wave Initiation in Large-Aspect-Ratio Channels," *AIAA Journal*, Vol. 44, No. 10, 2006, pp. 2422–2425.

[18]Frederick, M. D., Gejji, R., Shepherd, J. E., and Slabaugh, C. D., "Preliminary Results from Narrow Channel Facility Experiments at Purdue University," *AIAA Propulsion and Energy Forum*, 2019.

[19]Lee, J. H. and Radulescu, M. I., "On the hydrodynamic thickness of cellular detonations," *Combustion, Explosion and Shock Waves*, Vol. 41, No. 6, 2005, pp. 745–765.

[20]Maxwell, B. M. N., Bhattacharjee, R. R., Lau-Chapdelaine, S. S., Falle, S. A., Sharpe, G. J., and Radulescu, M. I., "Influence of turbulent fluctuations on detonation propagation," *Journal of Fluid Mechanics*, Vol. 818, may 2017, pp. 646–696.

[21]Kiyanda, C. B. and Higgins, A. J., "Photographic investigation into the mechanism of combustion in irregular detonation waves," *Shock Waves*, Vol. 23, mar 2013, pp. 115–130.

[22]Schwinn, K., Gejji, R., Kan, B., Sardeshmukh, S., Heister, S., and Slabaugh, C. D., "Self-sustained, high-frequency detonation wave generation in a semi-bounded channel," *Combustion and Flame*, Vol. 193, 2018, pp. 384–396.

[23]Stechmann, D. P., Sardeshmukh, S., Heister, S. D., and Mikoshiba, K., "Role of Ignition Delay in Rotating Detonation Engine Performance and Operability," *Journal of Propulsion and Power*, Vol. 35, No. 1, 2019, pp. 125–140.

[24]Bennewitz, J. W., Bigler, B. R., Pilgram, J. J., and Hargus, W. A., "Modal Transitions in Rotating Detonation Rocket Engines," *International Journal of Energetic Materials and Chemical Propulsion*, Vol. 18, No. 2, 2019, pp. 91–109.

[25]Walters, I. V., Journell, C. L., Lemcherfi, A., Gejji, R. M., Heister, S. D., and Slabaugh, C. D., "Operability of a Natural Gas–Air Rotating Detonation Engine," *Journal of Propulsion and Power*, Vol. 36, No. 3, 2020, pp. 453–464.

[26]Walters, I. V., Lemcherfi, A., Gejji, R. M., Heister, S. D., and Slabaugh, C. D., "Performance Characterization of a Natural Gas–Air Rotating Detonation Engine," *Journal of Propulsion and Power*, 2020.

[27]Journell, C. L., Gejji, R. M., Walters, I. V., Lemcherfi, A. I., Slabaugh, C. D., and Stout, J. B., "High-Speed Diagnostics in a Natural Gas–Air Rotating Detonation Engine," *Journal of Propulsion and Power*, Vol. 36, No. 4, 2020, pp. 498–507.

[28]Zipf, R. K., Gamezo, V. N., Mohamed, K. M., Oran, E. S., and Kessler, D. A., "Deflagration-to-detonation transition in natural gas–air mixtures," *Combustion and Flame*, Vol. 161, No. 8, 2014, pp. 2165 – 2176.

[29]Prakash, S., Raman, V., Lietz, C., Hargus, W., and Schumaker, S., "Numerical simulation of a methane-oxygen rotating detonation rocket engine," *Proceedings of the Combustion Institute*, 2020.

[30]Shepherd, J. E., "Shock and Detonation Toolbox," 2018, https://shepherd.caltech.edu/EDL/PublicResources/sdt/.

[31]Radulescu, M. I., "A detonation paradox: Why inviscid detonation simulations predict the incorrect trend for the role of instability in gaseous cellular detonations?" *Combustion and Flame*, Vol. 195, sep 2018, pp. 151–162.

[32]Oran, E. S., Young, T. R., Boris, J. P., Picone, J. M., and Edwards, D. H., "A study of detonation structure: The formation ofunreacted gas pockets," *Symposium (International) on Combustion*, Vol. 19, No. 1, jan 1982, pp. 573–582.

[33]Subbotin, V. A., "Collision of transverse detonation waves in gases," *Combustion, Explosion, and Shock Waves*, Vol. 11, No. 3, may 1975, pp. 411–414.

[34]Massa, L., Austin, J. M., and Jackson, T. L., "Triple-point shear layers in gaseous detonation waves," *Journal of Fluid Mechanics*, Vol. 586, sep 2007, pp. 205–248.

[35]Arienti, M. and Shepherd, J. E., "The role of diffusion at shear layers in irregular detonations," *4th Joint Meeting of the US Sections of the Combustion Institute*, 2005.

[36]Kass, M. and Witkin, A., "Snakes: Active Contour Models," Tech. rep., 1988.

[37]Savitzky, A. and Golay, M. J., "Smoothing and Differentiation of Data by Simplified Least Squares Procedures," *Analytical Chemistry*, Vol. 36, No. 8, 1964, pp. 1627–1639.

[38]Fisher, R. A., "The Moments of the Distribution for Normal Samples of Measures of Departure from Normality," *Proceedings of The Royal Society A*, dec 1930, pp. 16–28.